RESEARCH ARTICLE

Noncanonical G-Protein-Dependent Modulation of Osteoclast Differentiation and Bone Resorption Mediated by *Pasteurella multocida* Toxin

Julia Strack,[a] Hannah Heni,[a] Ralf Gilsbach,[b] Lutz Hein,[b] Klaus Aktories,[a,c] Joachim H. C. Orth[a]

Department I[a] and Department II,[b] Institut für Experimentelle und Klinische Pharmakologie und Toxikologie, Albert-Ludwigs-Universität Freiburg, Freiburg, Germany; BIOSS Centre for Biological Signalling Studies, Universität Freiburg, Freiburg, Germany[c]

ABSTRACT ***Pasteurella multocida*** **toxin (PMT) induces atrophic rhinitis in animals, which is characterized by a degradation of nasal turbinate bones, indicating an effect of the toxin on bone cells such as osteoblasts and osteoclasts. The underlying molecular mechanism of PMT was defined as a persistent activation of heterotrimeric G proteins by deamidation of a specific glutamine residue. Here, we show that PMT acts directly on osteoclast precursor cells such as bone marrow-derived CD14$^+$ monocytes and RAW246.7 cells to induce osteoclastogenesis as measured by expression of osteoclast-specific markers such as tartrate-resistant acid phosphatase and bone resorption activity. Treatment performed solely with PMT stimulates osteoclast differentiation, showing a receptor activator of nuclear factor-κB ligand (RANKL)-independent action of the toxin. The underlying signal transduction pathway was defined as activation of the heterotrimeric G proteins G$\alpha_{q/11}$ leading to the transactivation of Ras and the mitogen-activated protein kinase pathway. G$\alpha_{q/11}$ transactivates Ras via its effector phospholipase Cβ-protein kinase C (PKC) involving proline-rich tyrosine kinase 2 (Pyk2). PMT-induced activation of the mitogen-activated protein kinase pathway results in stimulation of the osteoclastogenic transcription factors AP-1, NF-κB, and NFATc1. In addition, Ca^{2+}-dependent calcineurin activation of NFAT is crucial for PMT-induced osteoclastogenesis. The data not only elucidate a rationale for PMT-dependent bone loss during atrophic rhinitis but also highlight a noncanonical, G-protein-dependent pathway toward bone resorption that is distinct from the RANKL-RANK pathway but mimics it. We define heterotrimeric G proteins as as-yet-underestimated entities/players in the maturation of osteoclasts which might be of pharmacological relevance.**

IMPORTANCE ***Pasteurella multocida*** **toxin (PMT) induces degradation of nasal turbinate bones, leading to the syndrome of atrophic rhinitis. Recently, the molecular mechanism and substrate specificity of PMT were identified. The toxin activates heterotrimeric G proteins by a covalent modification. However, the mechanism by which PMT induces bone degradation is poorly understood. Our report demonstrates a direct effect of PMT on osteoclast precursor cells, leading to maturation of bone-degrading osteoclasts. Interestingly, PMT stimulates osteoclastogenesis independently of the cytokine RANKL, which is a key factor in induction of osteoclast differentiation. This implicates a noncanonical osteoclastogenic signaling pathway induced by PMT. The elucidated G$\alpha_{q/11}$-dependent osteoclastogenic signal transduction pathway ends in osteoclastogenic NFAT signaling. The noncanonical, heterotrimeric G protein-dependent osteoclast differentiation process may be of pharmacological relevance, as members of this pathway are highly druggable. In particular, modulation of G protein-coupled receptor activity in osteoclast progenitors by small molecules might be of specific interest.**

Received 23 October 2014 **Accepted** 24 October 2014 **Published** 11 November 2014

Citation Strack J, Heni H, Gilsbach R, Hein L, Aktories K, Orth JHC. 2014. Noncanonical G-protein-dependent modulation of osteoclast differentiation and bone resorption mediated by *Pasteurella multocida* toxin. mBio 5(6):e02190-14. doi:10.1128/mBio.02190-14.

Editor Stephen Carlyle Winans, Cornell University

Address correspondence to Joachim H. C. Orth, Joachim.Orth@pharmakol.uni-freiburg.de, or Klaus Aktories, Klaus.Aktories@pharmakol.uni-freiburg.de.

This article is a direct contribution from a Fellow of the American Academy of Microbiology.

Pasteurella multocida is a facultative pathogenic commensal which is important for causing various diseases in animals and humans (1). *P. multocida* toxin (PMT), produced by serotype D and some serotype A strains, is the causative agent of atrophic rhinitis, which is characterized by the loss of nasal turbinate bones, implicating an effect of the *P. multocida* infection on bone cells (2–4). It was earlier shown that PMT stimulates osteoclastic bone resorption (5, 6). However, the exact molecular mechanism and the underlying signaling remained enigmatic. Previous work from our laboratory elucidated the primary action of PMT as the activation of heterotrimeric G proteins. Of the four major families of heterotrimeric G proteins, PMT activates Gα_{i1-3}, G$\alpha_{q/11}$, and G$\alpha_{12/13}$ but not Gα_s (7). The molecular mechanism of G protein activation by PMT is the deamidation of a conserved glutamine residue in the switch II region of the α-subunit of heterotrimeric G proteins (8). This glutamine residue is critical for the inactivation reaction, i.e., hydrolysis of GTP by the G protein (9). Therefore, PMT-induced deamidation leads to a permanent activation of heterotrimeric G proteins. As a consequence, PMT overcomes the tight regulation of endogenous signaling by heterotrimeric G proteins.

Bone is a dynamic tissue, consisting of specialized cells, osteoblasts and osteoclasts, that are engaged in continuous regeneration, remodelling, and maintenance of bone tissue (10). Dysregulation of osteoclasts or osteoblast activities causes diseases such as osteoporosis or osteopetrosis. Moreover, bone destruction can be due to the presence of pathogenic bacteria, which can directly affect bone cells or release factors to indirectly target the skeleton system (11). Osteoclasts are multinuclear giant cells that are differentiated from the hematopoietic cells, i.e., monocyte/macrophage-lineage precursor cells (12). RANKL (receptor activator of nuclear factor-κB ligand) plays an essential role in osteoclastogenesis. It is produced by various cells such as osteoblasts, bone marrow stromal cells, and also osteocytes (13). RANKL binds to the RANK (receptor activator of nuclear factor-κB) osteoclast surface receptor and stimulates various signaling cascades. TRAF6 (tumor necrosis factor receptor-associated protein 6) and Gab-2 (Grb-associated binder-2) are RANK-interacting proteins and crucial for RANK signaling (4). These adaptor proteins stimulate activation of several signaling molecules such as mitogen-activated protein (MAP) kinases, Akt kinase, or PI3 kinases, leading to stimulation of transcription factors such as AP-1 and NF-κB (14). Finally, RANKL, in concert with additional factors, induces NFATc1 activation (15–18). Another key factor for NFAT activity is the interaction with calcineurin, which is controlled by Ca^{2+}/calmodulin (14). NFATc1 activation was recognized as an essential step for proper osteoclastogenesis (16). Control of osteoclastogenesis has been linked to paracrine signaling, such as parathyroid hormone stimulation of G protein-coupled receptors (GPCR) on osteoblasts, which can lead to an increase in RANKL levels over osteoprotegerin levels (19, 20). Proinflammatory cytokines such as interleukin-1β (IL-1β) or tumor necrosis factor (TNF) increase RANKL expression and thereby promote bone resorption (21). However, regulation or fine-tuning of osteoclastogenesis via other signaling cascades—especially in osteoclasts—is not well understood.

Here, we show that PMT directly affects bone marrow cells and, especially, osteoclast precursors, leading to osteoclast maturation. By activation of heterotrimeric G proteins, the MAP kinase pathway is transactivated and transcription factors essential for osteoclastogenesis are stimulated. Additionally, Ca^{2+}-dependent calcineurin interaction with NFAT is required for PMT-stimulated osteoclastogenesis. Our results highlight the importance of G protein signaling in osteoclastogenesis and open perspectives for new therapeutic principles in osteoclast dependent diseases.

(Parts of the work were included in the doctoral thesis of J. Strack.)

RESULTS

PMT induces osteoclastogenesis. The bone-degrading phenotype of PMT intoxication can be explained by noting that it affects differentiation and activity of specialized bone cells such as osteoblasts and osteoclasts. In addition to the inhibitory effect of PMT on osteoblasts (22), osteoclasts might be of major importance because of the observed strong and fast depletion of bone matrix. To identify osteoclast precursor cells as direct targets of PMT, we used isolated primary bone marrow-derived $CD14^+$ monocytes and cultured RAW246.7 cells, a $CD14^+$ monocyte-like cell line (see Fig. S1 in the supplemental material). These $CD14^+$ monocytes give rise to macrophages or osteoclasts, depending on the culture conditions (12), and RAW246.7 cells are a frequently used cell culture model to analyze osteoclast differentiation (23). To demonstrate that PMT deamidates G proteins in these cells, we analyzed PMT-induced deamidation of heterotrimeric G proteins (Fig. 1A and B). PMT-induced deamidation can be directly monitored by immunoblot analysis using a recently described antibody which recognizes only the deamidated form of heterotrimeric Gα proteins (24). As osteoclast progenitor cells originate from the bone marrow, we investigated whether PMT is able to reach this compartment. We intraperitoneally administered PMT or the biological inactive mutant PMT^{C1165S} to mice. After 72 h, bone marrow cells were prepared and checked for intoxication. As shown in Fig. 1C, catalytically active PMT but not PMT^{C1165S} led to a deamidation of heterotrimeric G proteins in bone marrow-derived cells. This indicates that the toxin spreads to this compartment, leading to the proposition that PMT acts far from the infection site (Fig. 1C).

To study the effect of PMT on osteoclast differentiation, we utilized RAW246.7 cells. Treatment of RAW246.7 cells with RANKL led to expression of tartrate-resistant acid phosphatase (TRAP), a specific marker of osteoclasts (16). As shown in Fig. 1D, TRAP was stained using an enzyme-linked fluorescence 97 (ELF 97) kit. PMT stimulated TRAP expression after incubation for 6 days (Fig. 1D). However, cells left untreated or incubated with the inactive enzymatic mutant of PMT (PMT^{C1165S}), which is not capable of activating G proteins by deamidation, did not induce TRAP formation. Additionally, $CD14^+$ monocytes were treated with RANKL or PMT or left untreated for 6 days. RANKL and PMT strongly induced TRAP expression (Fig. 1E). Quantification of TRAP-positive cells showed the same levels of induction by PMT and RANKL. Moreover, formation of multinucleated cells, another hallmark of osteoclastogenesis (25), was stimulated by PMT and RANKL (Fig. 1F).

Signaling cascades induced by PMT. Next we compared the effect of PMT with that of RANKL, which acts via RANK to induce the MAP kinase pathway and to activate gene transcription, resulting in differentiation of osteoclast progenitor cells (15). We found comparable activation patterns induced by RANKL and PMT. Two members of the MAP kinases are c-Jun N-terminal kinase (JNK) and extracellular-regulated kinase 1/2 (ERK1/2). Both were activated by incubation of RAW246.7 cells with RANKL as shown by phosphorylation-specific immunoblot analysis. RANKL acts via the RANK receptor, leading to fast activation of downstream signaling cascades. Stimulation was detectable after just 25 min of treatment with RANKL. PMT, but not the inactive PMT^{C1165S}, induced JNK and ERK1/2 activation (Fig. 2A). As the action of PMT depends on cellular uptake, toxin-induced signaling occurs with a delay. Interestingly, PMT-induced signaling persisted at least for 24 h (Fig. 2B), which is in line with the persistent activation of heterotrimeric G proteins. Because Ras activity is of major importance for the regulation of downstream MAP kinases (26), we analyzed the effect of PMT treatment on the Ras activation level. As measured by effector pulldown experiments of active Ras, we detected strong transactivation of Ras by PMT but not by PMT^{C1165S} (Fig. 2C).

Stimulation of transcription factors such as AP-1, NF-κB, or NFATc1 is essential for induction of osteoclast differentiation (16–18). RANKL stimulated all three transcription factors in a dual-luciferase assay system. PMT induced transcriptional activity of the tested transcription factors, whereas the inactive PMT

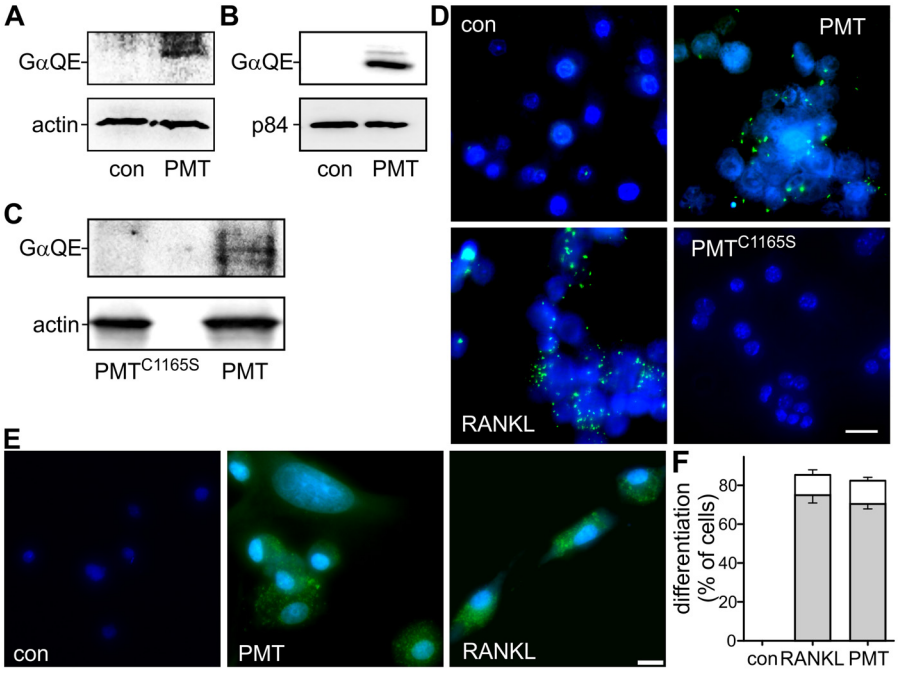

FIG 1 Susceptibility of osteoclast precursor cells to PMT. (A to C) Immunoblot analyses were performed with deamidation-specific antibody (GαQE). Loading control: actin (bone marrow-derived cells and $CD14^+$ cells) or nuclear matrix protein p84 (RAW246.7). (A and B) Primary $CD14^+$ (A) and RAW246.7 (B) cells were treated with PMT (1 nM) for 20 h or left untreated as a control (con). PMT deamidates various α-subunits of heterotrimeric G proteins ranging in size between 40 and 43 kDa; therefore, multiple bands can appear in PMT-treated samples. (C) Mice were injected intraperitoneally with PMT or PMT^{C1165S} (each at 500 ng/kg of body weight). After 72 h, bone marrow cells were prepared. PMT-induced deamidation of heterotrimeric G proteins was detected by immunoblotting with anti-GαQE antibody ($n = 3$). (D and E) Osteoclast differentiation of osteoclast precursor cells by PMT. RAW246.7 cells (D) or bone marrow-derived $CD14^+$ cells (E) were incubated with PMT or PMT^{C1165S} (each at 1 nM) or RANKL (35 ng/ml) for 6 days. Expression of an osteoclast-specific marker, TRAP, was shown by enzyme-linked fluorescence. TRAP is depicted in green and nuclei in blue. The scale bars indicate 10 μm ($CD14^+$) and 20 μm (RAW246.7). (F) Quantification of PMT-induced osteoclastogenesis in $CD14^+$ monocytes as shown in panel E. TRAP-positive cells and multinuclear cells were counted (white, multinucleated TRAP-positive [$TRAP^+$] cells; gray, $TRAP^+$ cells). Images of 3 independent experiments were analyzed, and data are given as ± standard errors of the means (SEM).

mutant exhibited no stimulation (Fig. 2D to F). Moreover, we analyzed the concentration-dependent activity of the transcription factors. These results show the high potency of PMT with respect to induction of AP-1, NF-κB, and NFATc1 activity. Incubation of cells with low concentrations (10 to 100 pM) of PMT effectively stimulated these transcription factors.

In addition, we studied the influence of NFAT and calcineurin activity on PMT-induced osteoclastogenesis. Inhibition of calcineurin interaction with NFAT performed using the cell-permeative inhibitor MCV1 clearly blocked RANKL- and PMT-induced TRAP expression (Fig. 3). These data indicate that NFATc1 activity and the interaction with the Ca^{2+}-dependent calcineurin pathway are crucial not only for RANKL but also for PMT-induced osteoclastogenesis.

In the pathogenesis of atrophic rhinitis, PMT should act on osteoclasts concomitantly with RANKL, which is probably present at physiological levels. Therefore, we studied the effect of PMT and RANKL together on NFATc1 activity. Different concentrations of PMT were used to stimulate NFATc1 transcriptional activity. RANKL alone stimulated NFATc1 only marginally, and a combination of RANKL with a high concentration (100 pM) of PMT did not enhance the strong signal of PMT. However, addition of RANKL to a low concentration (10 pM) of PMT led to a more-than-additive effect on NFATc1-dependent transcription (Fig. 3B).

Heterotrimeric G proteins and osteoclastogenesis. Recent reports showed that the toxin activates the $G\alpha_{i1\text{-}3}$, $G\alpha_{q/11}$, and $G\alpha_{12/13}$ family of heterotrimeric G proteins, whereas $G\alpha_s$ is not susceptible to PMT action (7). The activated α-subunits led to stimulation of various signaling cascades (27). To elucidate the basis of the effect of the toxin on osteoclastogenesis, the relevant PMT-induced signaling cascades were studied in detail.

First, the heterotrimeric G protein families were analyzed for their contribution to PMT-stimulated NFATc1 activity. For the analysis, different regulators of G protein signaling (RGS) proteins were ectopically expressed in RAW246.7 cells. RGS proteins enhance the inherent GTPase activity of Gα, leading to faster inactivation of G protein signaling (28). Moreover, they are able to compete with the effectors of Gα to block signaling (29). To differentiate between the G protein families, we utilized Lsc-RGS and RGS2 and the RGS domain of G protein-coupled receptor kinase 2 (GRK2). Lsc-RGS couples to $G\alpha_{12/13}$, RGS2 blocks $G\alpha_{q/11}$ and $G\alpha_i$ signaling, and RGS-GRK2 specifically interacts with the $G\alpha_{q/11}$ family (30, 31). PMT-induced NFATc1 activity was not affected by Lsc-RGS, but ectopic expression of RGS2 or RGS-GRK2, each interacting with $G\alpha_{q/11}$, diminished the effect of PMT (Fig. 4A). Our results showed that $G\alpha_{q/11}$ signaling is essential for PMT-stimulated NFATc1 activity. These results were corroborated by utilizing YM-254890, a specific inhibitor of $G\alpha_{q/11}$. This compound is a cyclic depsipeptide from *Chromobacterium*, and

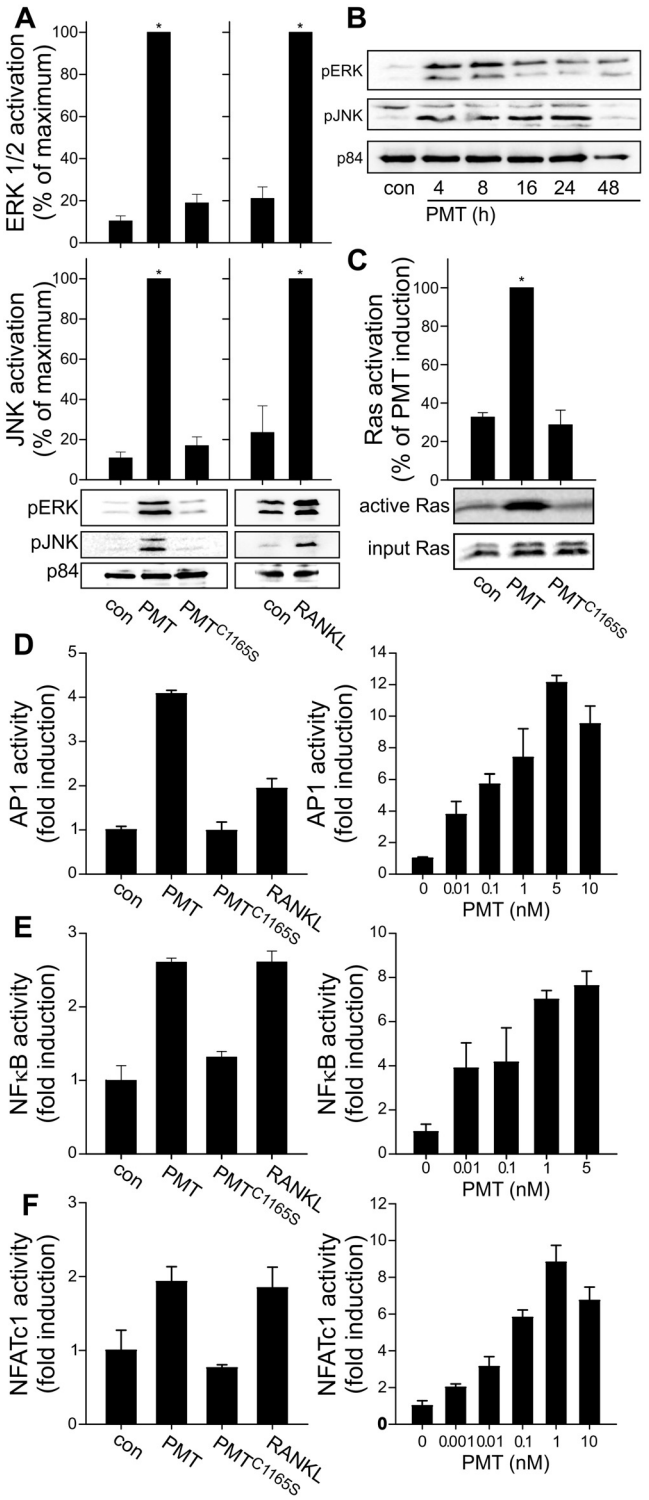

FIG 2 PMT-activated signal transduction pathways related to RANKL-induced osteoclastogenesis. (A) Immunoblot of pERK/2, pJNK, or p84 as a loading control. RAW246.7 cells were treated with PMT or PMT^{C1165S} (each 1 nM) for 20 h or with RANKL (35 ng/ml) for 25 min or left untreated as a control (con). (B) Time-dependent activation of ERK1/2 and JNK by PMT. RAW246.7 cells were incubated with PMT (1 nM) for the indicated times. (C) Effector pulldown assay of activated Ras. RAW246.7 cells were incubated with or without PMT or PMT^{C1165S} (1 nM) for 4 h. An immunoblot of precipitated Ras is shown. Quantification was performed using MultiGauge and demonstrated as the portion of maximum induction ± SEM ($n \geq 3$). (D, E, and F) *(Continued)*

several reports show that only the G$\alpha_{q/11}$ family of heterotrimeric G proteins is affected (32, 33). Treatment of RAW246.7 cells with YM-254890 blocked PMT-induced NFATc1 activity (Fig. 4B). We next focused on the issue of which G$\alpha_{q/11}$ effector transduces the signal to NFATc1 activation. Well-known effectors of G$\alpha_{q/11}$ are p63RhoGEF and phospholipase Cβ (PLCβ). Recently, it was reported that p63RhoGEF-induced RhoA activation is important for PMT-derived inhibition of osteoblastogenesis by transactivation of the MAP kinase cascade (22). However, p63RhoGEF has a restricted tissue expression profile (34) and we were not able to detect p63RhoGEF expression in RAW246.7 cells (see Fig. S2 in the supplemental material). Additionally, in these osteoclast progenitor cells, PMT-induced RhoA activation was not dependent on G$\alpha_{q/11}$ signaling alone, as inhibition of G$\alpha_{q/11}$ by YM-254890 did not hamper RhoA activation (see Fig. S2). The other effector, PLCβ, stimulates expression of protein kinase C (PKC) via formation of diacylglycerol (DAG) (35). Pharmacological inhibition of PKC (GF109203X) efficiently blocked PMT-induced NFATc1 activity, indicating that the canonical G$\alpha_{q/11}$-PLCβ-PKC pathway transfers the PMT effect (Fig. 4B).

PMT and RANKL potently induce mitogen-activated protein kinase (MAPK) signaling, as demonstrated by phosphorylation of ERK1/2 and JNK. That MAPK signaling is critical for PMT-stimulated NFATc1 transcriptional activity was shown by inhibition of MEK-1, the kinase upstream of ERK1/2. Treatment of RAW246.7 cells with MEK-1 inhibitor PD98059 completely abolished NFATc1 activity (Fig. 4B).

This result prompted us to study the signaling cascade of Ras activation by PMT in detail. Receptor tyrosine kinase-independent stimulation of Ras can be evoked by different factors (36), and additional tyrosine kinases such as proline-rich tyrosine kinase 2 (Pyk2) and/or Src may be involved in heterotrimeric G protein-dependent transactivation of Ras (37, 38). Moreover, Pyk2 has been implicated in proper osteoclast differentiation by binding to cSrc and the Traf6-RANK complex (39, 40). We could demonstrate the stimulation of Pyk2 by PMT but not by PMT^{C1165S} (Fig. 4C). Moreover, a short hairpin RNA (shRNA)-mediated knockdown of Pyk2 diminished PMT-induced MAPK activation as measured by ERK1/2 phosphorylation, indicating a contribution of Pyk2 to transactivation of the MAPK pathway (Fig. 4D).

Additionally, a direct measurement of the activation status of Ras was performed with an effector pulldown assay. Pharmacological inhibition of G$\alpha_{q/11}$ by YM-254890 and of its downstream effector PKC by GF109203X and blockade of Src kinase by PP2 abolished PMT-induced Ras activity (see Fig. S2 in the supplemental material). Also, inhibition of Src kinase blocked PMT-induced NFATc1 activity (Fig. 4B).

G$\alpha_{q/11}$ is important for osteoclastogenesis induced by PMT. To support our results indicating that G$\alpha_{q/11}$ is of pivotal importance in PMT-induced osteoclastogenesis, we studied its contribution to differentiation. We utilized CD14$^+$ monocytes and in-

Figure Legend Continued

PMT and RANKL stimulate AP-1-, NF-κB-, and NFATc1-dependent transcriptional activation as measured by luciferase expression. Cells were treated with PMT or PMT^{C1165S} (each at 1 nM) or with RANKL (50 ng/ml) for 20 h (left panels) or with the indicated concentrations of PMT (right panels). Data represent the fold stimulation of luciferase compared with control results. Experiments were performed at least three times with similar results.

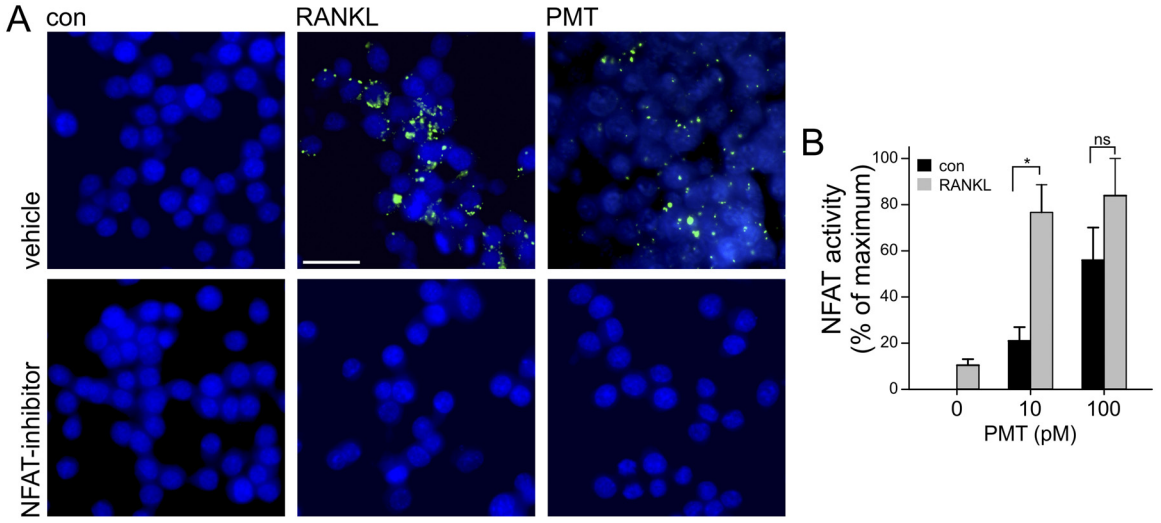

FIG 3 NFATc1 activity is essential for PMT-induced osteoclastogenesis. (A) RAW246.7 cells were differentiated with RANKL (50 ng/ml) or PMT (100 pM) or left untreated (con). After 8 days, TRAP was stained with ELF 97 as a marker of osteoclastogenesis. Samples treated with an inhibitor of NFAT (MCV1; 100 nM) exhibited no TRAP staining. TRAP is depicted in green and nuclei in blue. The scale bar indicates 20 μm. Experiments were performed at least three times with similar results. (B) PMT and RANKL act synergistically at submaximal concentrations on NFATc1 transcriptional activity. RAW246.7 cells were treated solely with RANKL (50 ng/ml) or in combination with the indicated concentrations of PMT. NFATc1 activity was calculated as the percentage of maximum activation ± SEM ($n \geq 3$).

duced osteoclastogenesis by PMT and determined differentiation results by analysis of TRAP formation. As expected, inhibition of $G\alpha_{q/11}$ signaling by YM-254890 completely blocked PMT-dependent differentiation (Fig. 5A and B). Interestingly, RANKL-induced osteoclastogenesis was also hampered by inhibition of $G\alpha_{q/11}$. These results provide strong evidence that PMT-stimulated osteoclastogenesis mainly depends on $G\alpha_{q/11}$. In the case of the physiological osteoclastogenic factor RANKL, $G\alpha_{q/11}$ is not essential but contributes to differentiation.

The major feature of mature osteoclasts is the ability to degrade bone matrix. To test whether the differentiation induced by PMT led to formation of proper osteoclasts, we cultivated $CD14^+$ monocytes on an artificial bone matrix and analyzed matrix resorption after 14 days. As shown in Fig. 4C, when cultivated cells were treated with PMT, the surface exhibited resorption lacunae. Equivalent results were observed after RANKL-induced differentiation. This result is a strong indication that PMT is able to stimulate differentiation of $CD14^+$ monocytes, leading to functional osteoclasts. Moreover, cocultivation of $CD14^+$ monocytes with PMT and the inhibitor of $G\alpha_{q/11}$ completely blocked bone matrix degradation, supporting the idea of an essential role for $G\alpha_{q/11}$ in PMT-dependent osteoclastogenesis (Fig. 5C and D).

DISCUSSION

Tight regulation and interaction of osteoblasts and osteoclasts are essential to maintenance of the structure and functions of bone tissue. *Pasteurella multocida* toxin (PMT) disturbs this functional balance. The toxin is the causative agent of atrophic rhinitis, which is primarily characterized by the degradation of nose turbinate bones (4, 41). This effect is most likely based on enhanced bone resorption by osteoclasts and a lack of bone regeneration by osteoblasts. Recently, we identified the PMT-sensitive signaling pathway involved in differentiation of preosteoblasts. Stimulation of this pathway by PMT prevents osteoblast development and eventually blocks new bone formation (22). However, it has been suggested that the harsh degradation of bone matrix by PMT predominantly depends on the stimulated activity of osteoclasts, whereas the blockade of osteoblasts enhances this effect. Therefore, we analyzed the PMT-induced effects on osteoclast precursor cells in detail. PMT treatment of osteoclast precursor cells stimulated maturation of functional osteoclasts as measured by expression of TRAP and resorption activity.

Mullan et al. detected differentiation of osteoclasts by PMT in a coculture model of osteoblasts and preosteoclasts. Based on the coculture system, it was not possible to clarify whether PMT acts directly on osteoclast precursor cells (42). More recently, it was proposed that the effect of PMT on osteoclast differentiation results from changes in the lymphoid system and expression of stimulatory cytokines such as IL-1β, IL-6, TNF-α, or RANKL by B cells rather than from a direct effect on osteoclast precursor cells (43). Here, we demonstrate that PMT is able to act directly on isolated bone marrow-derived $CD14^+$ monocytes as shown by toxin-specific deamidation of heterotrimeric G proteins. Moreover, PMT efficiently stimulated osteoclastic differentiation of $CD14^+$ cells without any further addition of cytokines. These results clearly show that PMT acts directly on osteoclast precursor cells. Osteoclast precursor cells originate from the hematopoietic lineage in the bone marrow. By detecting the primary molecular action of PMT in bone marrow-derived cells after intraperitoneal injection, we were able to demonstrate that the toxin spreads to this compartment, suggesting that the toxin acts not only at locations close to the infection site.

We next compared the toxin effect with that of RANKL, the well-known inducer of osteoclast differentiation (13). Surprisingly, we found comparable activation patterns induced by RANKL and PMT. PMT stimulated Ras and, as known for RANKL (15), the MAPK pathway. Like RANKL (14, 16–18), PMT increased the transcriptional activity of NF-κB, AP-1, and NFATc1. Moreover, in agreement with the essential role of

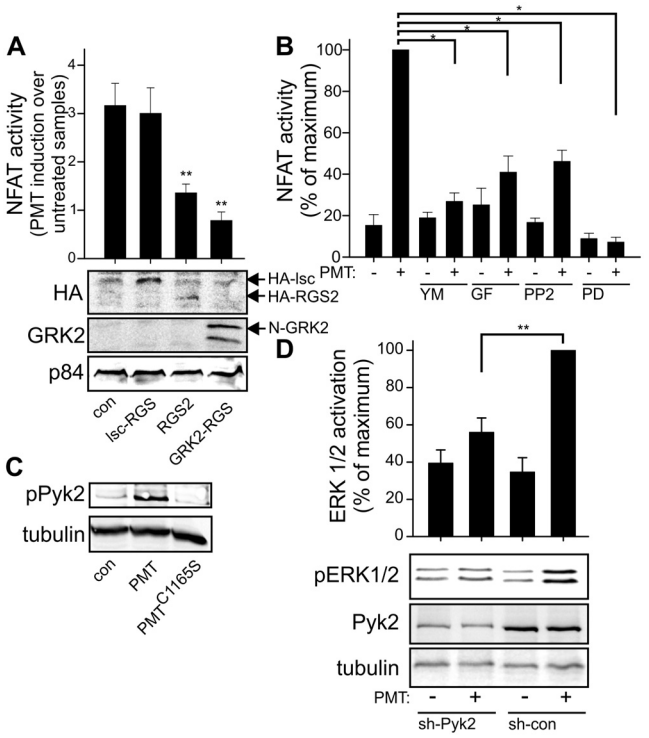

FIG 4 PMT-induced signaling cascade to stimulate osteoclastogenesis. (A) Inhibition of heterotrimeric G protein signaling by overexpression of RGS proteins. NFATc1 activity was measured by the use of a dual-luciferase assay and calculated as fold induction over the results seen with untreated samples. Data represent immunoblots of PAGE gels from representative cell lysates, using anti-HA antibodies against HA-Lsc-RGS, HA-RGS2, and N-GRK2, with anti-p84 used as a loading control. (B) PMT-dependent NFATc1 transcriptional activity in the presence of the indicated inhibitor. Cells were treated with the indicated inhibitor (YM-254890, 10 μM; GF109203X, 10 μM; PP2, 5 μM; PD98059, 50 μM) and/or PMT (100 pM). Results are presented as percentages of the maximum activity ± SEM ($n \geq 3$). (C) Immunoblot of phosphorylated Pyk2. RAW246.7 cells were treated without or with PMT or PMT^{C1165S} (each 1 nM) for 4 h. Shown are immunoblots representative of the results of at least three experiments. (D) Immunoblots of pERK/2, Pyk2, and tubulin as a loading control. RAW246.7 cells were transduced with Pyk2-targeting or control shRNA (con-shRNA) followed by puromycin selection. Cells were treated with PMT (1 nM) or left untreated as a control (con) for 20 h, and lysates were prepared for immunoblot analysis. Quantification was calculated using MultiGauge and demonstrated as the portion of maximum induction ± SEM ($n = 3$).

NFATc1 in RANKL-induced osteoclastogenesis (44), inhibition of NFATc1 completely blocked PMT-dependent differentiation. Furthermore, blockade of MAPK signaling inhibited the transcriptional activity of NFATc1, indicating that the transactivation of the MAPK cascade is a crucial step in PMT-mediated osteoclastogenesis.

What is the mechanism of PMT-induced transactivation, and which factors are involved? PMT is known to activate the $G\alpha_i$, $G\alpha_{12/13}$, and $G\alpha_{q/11}$ family of heterotrimeric G proteins (7). By ectopic expression of RGS proteins, which specifically block subsets of G proteins (28), we identified $G\alpha_{q/11}$ as an essential player in PMT-induced osteoclastogenesis. The identification of the specific role of $G\alpha_{q/11}$ is corroborated by the finding that YM-254890, which selectively blocks $G\alpha_{q/11}$ (32, 33), inhibited the PMT effect on osteoclast differentiation.

Recently, we reported that PMT blocked differentiation of osteoblasts in a $G\alpha_{q/11}$-dependent manner via the MAPK cascade (22). This PMT-induced transactivation of the MAPK pathway and the subsequent inhibition of osteoblast differentiation depend on $G\alpha_{q/11}$-p63RhoGEF-induced RhoA/Rho-kinase activation (22). In osteoclast precursor cells, however, we failed to detect p63RhoGEF- and $G\alpha_{q/11}$-dependent RhoA activation (see Fig. S2 in the supplemental material), indicating the presence of a different signaling cascade. In contrast, our findings in osteoclasts suggested that PMT-induced transactivation of the Ras/MAPK pathway depended on the presence of the $G\alpha_{q/11}$ effector PKC. Activation of PKC has been implicated in transactivation of the MAPK cascade via the kinases Src and Pyk2 (38). In line with this report, we detected stimulation of Pyk2 by PMT. Moreover, a knockdown of Pyk2 diminished PMT-induced MAPK activation and inhibition of Src kinase blocked PMT-induced Ras activation. These findings suggest that in osteoclasts, PMT stimulates Ras by activating the $G\alpha_{q/11}$-PKC-Src/Pyk2 axis. In addition, it is well known that activation of $G\alpha_{q/11}$ by PMT also induces Ca^{2+} signaling, which is important for NFATc1 activity (16), via the PLCβ-IP_3 pathway (27, 45). Our data showing inhibition of PMT-induced osteoclastogenesis using MCV1, which blocks interaction of calcineurin with NFAT, indicate that, in addition to the MAPK pathway, Ca^{2+}-calmodulin-calcineurin signaling is crucial for PMT-stimulated osteoclastogenesis.

Whereas canonical signaling depends on the activity of RANKL on osteoclast precursor cells, RANKL can be substituted by other cytokines such as IL-6, IL-8, or TNF-α in noncanonical signaling pathways (46). However, heterotrimeric G proteins ($G\alpha/G\beta\gamma$) were detected only recently as players in the regulation of osteoclast differentiation, which stands in contrast to the extensive knowledge of heterotrimeric G protein signaling in osteoblasts (19, 47). One of the few examples is the influence of OGR1 (ovarian cancer GPCR 1) on the differentiation and/or activity of osteoclasts (48–50). Interestingly, OGR1 couples to heterotrimeric G proteins of the $G\alpha_q$ family to regulate osteoclastogenesis. In line with the regulation by heterotrimeric G protein signaling, a specific RGS protein (RGS18) in osteoclasts was previously described as a negative regulator of OGR1 signaling (51).

In summary, we have shown that PMT induces osteoclastogenesis by direct stimulation of the osteoclastogenic transcription program in preosteoclasts (Fig. 6). This effect is independent of RANKL but ends up in its signaling cascade. Furthermore, it is a potentially important finding that activation of $G\alpha_{q/11}$ is sufficient for osteoclastogenesis and that inhibition of $G\alpha_{q/11}$ by YM-254890 also affected osteoclast differentiation by RANKL. These effects indicate that signal transduction of heterotrimeric G proteins has a previously underestimated role in the differentiation of osteoclasts. Thus, our results may offer a new rationale for pharmacological treatment of osteoclast-dependent diseases via $G\alpha_{q/11}$-interacting GPCR.

MATERIALS AND METHODS

Reagents. Dulbecco's modified Eagle medium (DMEM) and fetal bovine serum (FBS) were obtained from Biochrom (Berlin, Germany). Recombinant murine soluble RANKL (sRANKL) was purchased from PeproTech (Hamburg, Germany). MCV1, a cell-permeative peptide inhibitor blocking calcineurin interactions with NFAT, was purchased from Millipore. An ELF 97 endogenous phosphatase detection kit, Opti-MEM, Lipofectamine 2000 transfection reagent, and Syto24 were purchased from Life Technology.

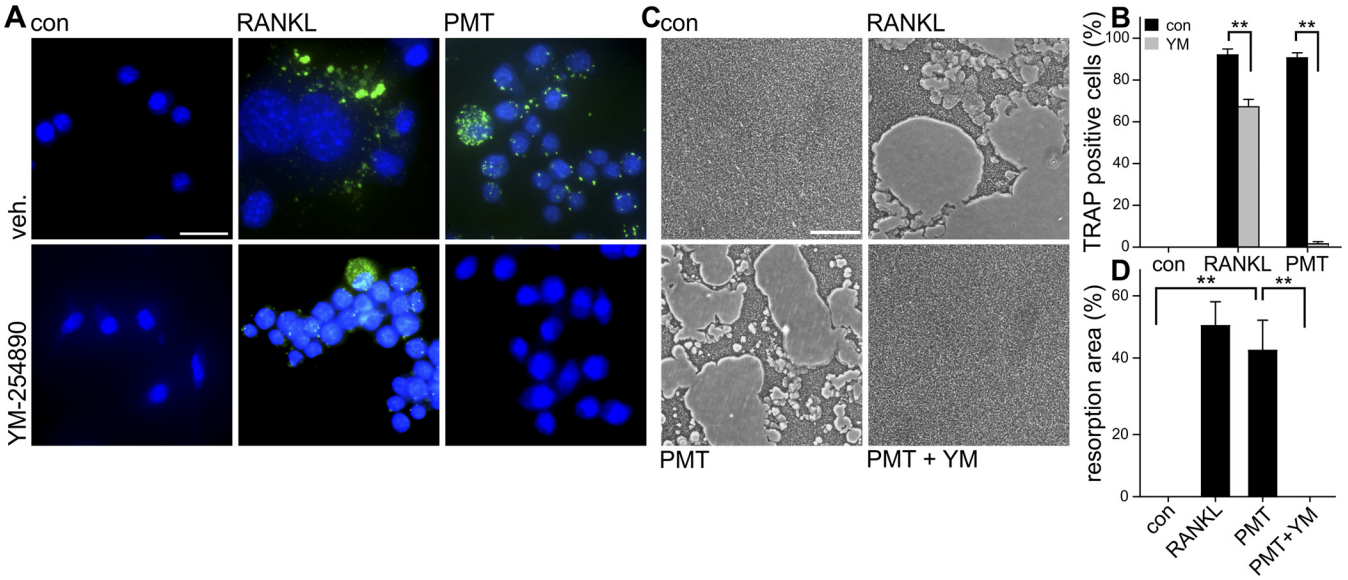

FIG 5 Inhibition of PMT-induced osteoclastogenesis. (A) CD14$^+$ cells were treated with PMT (100 pM) or RANKL (50 ng/ml) for 8 days. ELF-labeled TRAP is depicted in green and nuclei in blue. (B) Quantification of PMT-induced osteoclastogenesis in CD14$^+$ monocytes as shown in panel A. TRAP-positive cells were counted and quantified as the portion of all cells. (C) Resorption pit assay of CD14$^+$ cells. Cells were incubated without (con) or with PMT (100 pM) in the absence (PMT) or presence of YM-254890 (10 μM; PMT + YM). (D) Resorption areas were analyzed by differential interference contrast microscopy and quantified. At least 3 independent experiments were analyzed, and results are given as ± SEM. Scale bars indicate 20 μm.

Cells and differentiation. RAW264.7 cells were cultured in DMEM supplemented with 10% FBS and 1% penicillin-streptomycin. Murine bone marrow cells were isolated from the femurs of 6-to-10-week-old mice and separated to segregate CD14$^+$ cells by the use of a PluriBead kit (pluriSelect, Leipzig, Germany) according to the manufacturer's manual. Isolated CD14$^+$ cells were cultured in DMEM containing 10% FBS and 1% penicillin-streptomycin. For osteoclast differentiation, RAW264.7 cells were seeded on coverslips in a 24-well plate with a density of 2.85 × 10^5 cells per well. Cells were treated with 35 ng/ml RANKL or PMT or the inactive mutant PMT^{C1165S} at the indicated concentrations for 6 days. All samples were washed with phosphate-buffered saline (PBS) and fixed with 4% paraformaldehyde for 30 min. Fixed cells were subjected to TRAP staining with an ELF 97 endogenous phosphatase detection kit according to the manufacturer's instructions. In addition, the nuclei were stained with Syto24. Isolated CD14$^+$ cells were cultured on coverslips in a 24-well plate and treated with RANKL (35 ng/ml) or PMT (1 nM). After 6 days, TRAP staining with an ELF 97 endogenous phosphatase detection kit, in line with the manufacturer's instructions, was performed. In addition, the nuclei were stained with Syto24.

Resorption pit assay. CD14$^+$ cells were seeded in a 24-well Corning Osteo assay plate with a density of 1 × 10^6 cells per well. For differentiation, cells were treated with or without 100 pM PMT for 14 days, with a change of the medium on every second day. A resorption pit assay for osteoclasts was performed in line with the manufacturer's instructions. The resorption area was measured utilizing the MetaMorph Microscopy Software package.

Transfection. To knock down Pyk2, the mouse kinase activity GIPZ lentiviral microRNA-adapted short hairpin RNA gene family collection

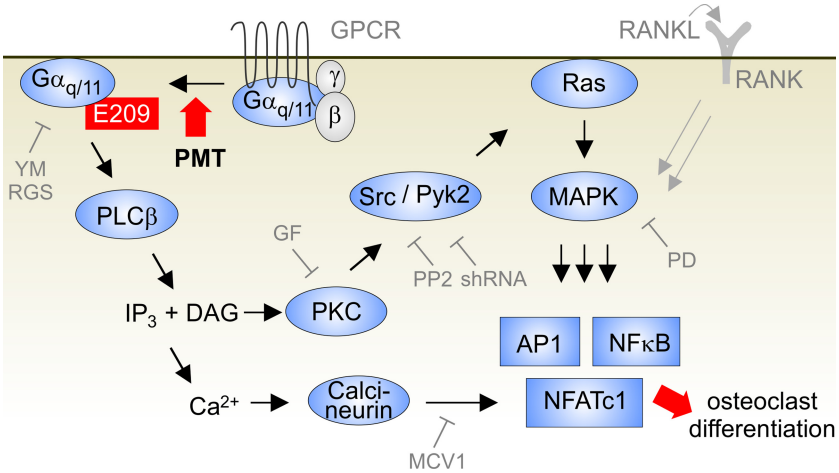

FIG 6 Scheme of PMT-induced signal transduction pathway to stimulate osteoclastogenesis. PMT constitutively activates heterotrimeric G proteins of the $G\alpha_{q/11}$ family by deamidation. Transactivation of Ras and the MAPK pathway is due to the presence of $G\alpha_{q/11}$ effectors PLCβ and PKC. Finally, transcription factors (AP-1, NF-κB, and NFATc1) are activated. For details, see the Discussion. YM, YM-254890; GF, GF109203X; PD, PD98059.

(Open Biosystems) was used. The constructs targeting Pyk2 (V2LMM_21947) and a nonsilencing control (Open Biosystems) were transduced into RAW246.7 cells followed by puromycin (3 μg/ml) selection.

Immunoblot analysis. To detect PMT-deamidated Gα proteins, RAW264.7 cells and CD14-positive cells were seeded in a 6-well plate with a density of 1.5×10^6 or 5.5×10^5 cells per well in the presence or absence of PMT (1 nM, 20 h). To detect phosphorylation of ERK1/2 and JNK, RAW264.7 cells were plated in a 6-well plate with a density of 1.5×10^6 per well and allowed to adhere overnight. Cells were then treated with PMT or PMT^{C1165S} (each at 1 nM) for 6 h. Afterward, cells were lysed with 200 μl radioimmunoprecipitation assay (RIPA) buffer (1 mM EDTA, 25 mM Tris, 150 mM NaCl, 1% [vol/vol] Triton X-100, 1% [wt/vol] sodium deoxycholate, pH 7.4) containing complete protease inhibitor (Roche) and phosphatase inhibitor cocktail 2 and 3 (Sigma) for 20 min on ice. Lysates were then incubated on an overhead shaker for 30 min at 4°C and centrifuged (14,000 rpm for 20 min) at 4°C. Samples were separated by SDS-PAGE and transferred to a polyvinylidene (PVDF) membrane. Deamidation-specific antibody anti-Gα_q Q209E (3G3) (24) was used to detect PMT-induced deamidation. Primary antibodies against pERK/2, pSARK/JNK, and pPyk2 were obtained from Cell Signaling (Frankfurt, Germany). p63RhoGEF antibody (51004) was from Proteintech. Equal loading of immunoblots was tested by detection of tubulin, actin, or p84. Monoclonal p84 antibody was purchased from ProSci Inc. (Poway, CA, USA), and actin and monoclonal anti-α-tubulin antibody were purchased from Sigma (Taufkirchen, Germany). Binding of the appropriate secondary antibody conjugated to horseradish peroxidase was visualized by an enhanced chemiluminescence system, using an LAS-3000 imaging system (Fujifilm, Düsseldorf, Germany).

Gene reporter assay. Activity of AP-1-, NF-κB-, or NFATc1-dependent protein expression was measured by the use of a dual-luciferase reporter assay system (Promega, Mannheim, Germany). RAW264.7 cells were seeded at 2.9×10^5 cells per well in a 24-well plate and allowed to adhere overnight. Cells were then incubated with a mixture of 0.5 μg of *Renilla* luciferase plasmid (pRL-TK; Promega) and 1.0 μg pAP1-Luc (Stratagene, Waldbronn, Germany), NF-κB (Stratagene), or NFAT (pGL3-NFAT; Addgene plasmid 17870 [deposited by Jerry Crabtree]) plasmid, 48 μl Lipofectamine 2000, and 1.2 ml Opti-MEM. After 5 h of incubation, the medium was changed to DMEM containing 10% FBS and antibiotics. RANKL and PMT were added at the indicated concentrations and incubated for another day. In the case of NFAT and cotransfection with RGS-encoding plasmids, PMT was incubated for 48 h with hemagglutinin-tagged RGS2 (HA-RGS2) and HA-lsc-RGS as described previously (52). The plasmid, encoding the RGS fragment of GRK2 (N-GRK2), was a kind gift of M. Lohse (University of Würzburg).

Effector pulldown assay. RAW264.7 cells were seeded at 8.7×10^6 per 10-cm-diameter dish and allowed to adhere overnight. After serum starvation for 24 h, cells were treated with or without YM-254890, GF109203X, and PP2 for 30 min prior incubation with PMT for a further 4 h. Thereafter, cells were lysed and Ras pulldown experiments were performed using a glutathione *S*-transferase (GST)-Raf fusion protein as described previously (53). Activated RhoA was precipitated using the RhoA-binding region of rhotekin (rhotekin pulldown) as described previously (52).

PMT expression. Wild-type PMT (PMT) and the catalytically inactive mutant PMT^{C1165S} were expressed and purified as described previously (54).

Statistics. Results are presented as means ± standard errors (SE). Significance was assessed by paired Student's *t* tests. *P* values of <0.05 were considered to represent statistical significance (*, $P < 0.05$; **, $P < 0.01$; ns, not significant). Multiple-group comparisons were analyzed by analysis of variance (ANOVA) followed by Student's *t* test.

Ethics statement. All animal experiments were performed in compliance with the German animal protection law (TierSchG). The animals were housed and handled in accordance with good animal practice as defined by FELASA (http://www.felasa.eu/) and the national animal welfare body GV-SOLAS (http://www.gv-solas.de). The animal welfare committees of the University of Freiburg as well as the local authorities (Regierungspräsidium Freiburg; licenses G-08/02, X-09/31S, and X-13/03A) approved all animal experiments.

SUPPLEMENTAL MATERIAL

Supplemental material for this article may be found at http://mbio.asm.org/lookup/suppl/doi:10.1128/mBio.02190-14/-/DCSupplemental.

Figure S1, PDF file, 0.6 MB.

Figure S2, PDF file, 0.4 MB.

ACKNOWLEDGMENTS

The study was financially supported by the Deutsche Forschungsgemeinschaft (DFG; grants OR218/1 and SFB746).

We thank Mitsuaki Ohta (Astellas Pharma Inc., Ibaraki, Japan) for YM-254890, K. Kubatzky (University of Heidelberg, Germany) for RAW264.7 cells, Y. Horiguchi (Osaka University, Japan) for deamidation-specific antibody, and Silke Fieber and Petra Bartholome for excellent technical assistance.

REFERENCES

1. **Wilson BA, Ho M.** 2013. *Pasteurella multocida*: from zoonosis to cellular microbiology. Clin. Microbiol. Rev. **26:**631–655. http://dx.doi.org/10.1128/CMR.00024-13.
2. **Sterner-Kock A, Lanske B, Uberschär S, Atkinson MJ.** 1995. Effects of the *Pasteurella multocida* toxin on osteoblastic cells *in vitro*. Vet. Pathol. **32:**274–279. http://dx.doi.org/10.1177/030098589503200309.
3. **Jutras I, Martineau-Doizé B.** 1996. Stimulation of osteoclast-like cell formation by *Pasteurella multocida* toxin from hemopoietic progenitor cells in mouse bone marrow cultures. Can. J. Vet. Res. **60:**34–39.
4. **Horiguchi Y.** 2012. Swine atrophic rhinitis caused by *Pasteurella multocida* toxin and Bordetella dermonecrotic toxin. Curr. Top. Microbiol. Immunol. **361:**113–129. http://dx.doi.org/10.1007/82_2012_206.
5. **Elling F, Pedersen KB.** 1985. The pathogenesis of persistent turbinate atrophy induced by toxigenic *Pasteurella multocida* in pigs. Vet. Pathol. **22:**469–474.
6. **Martineau-Doizé B, Caya I, Gagné S, Jutras I, Dumas G.** 1993. Effects of *Pasteurella multocida* toxin on the osteoclast population of the rat. J. Comp. Pathol. **108:**81–91. http://dx.doi.org/10.1016/S0021-9975(08)80230-7.
7. **Orth JH, Fester I, Siegert P, Weise M, Lanner U, Kamitani S, Tachibana T, Wilson BA, Schlosser A, Horiguchi Y, Aktories K.** 2013. Substrate specificity of *Pasteurella multocida* toxin for α subunits of heterotrimeric G proteins. FASEB J. **27:**832–842. http://dx.doi.org/10.1096/fj.12-213900.
8. **Orth JH, Preuss I, Fester I, Schlosser A, Wilson BA, Aktories K.** 2009. *Pasteurella multocida* toxin activation of heterotrimeric G proteins by deamidation. Proc. Natl. Acad. Sci. U. S. A. **106:**7179–7184. http://dx.doi.org/10.1073/pnas.0900160106.
9. **Coleman DE, Berghuis AM, Lee E, Linder ME, Gilman AG, Sprang SR.** 1994. Structures of active conformations of Gi alpha 1 and the mechanism of GTP hydrolysis. Science **265:**1405–1412. http://dx.doi.org/10.1126/science.8073283.
10. **Rodan GA.** 1992. Introduction to bone biology. Bone **13**(Suppl 1):S3–S6. http://dx.doi.org/10.1016/8756-3282(92)90468-C.
11. **Henderson B, Nair SP.** 2003. Hard labour: bacterial infection of the skeleton. Trends Microbiol. **11:**570–577. http://dx.doi.org/10.1016/j.tim.2003.10.005.
12. **Massey HM, Flanagan AM.** 1999. Human osteoclasts derive from CD14-positive monocytes. Br. J. Haematol. **106:**167–170. http://dx.doi.org/10.1046/j.1365-2141.1999.01491.x.
13. **Nakashima T, Hayashi M, Takayanagi H.** 2012. New insights into osteoclastogenic signaling mechanisms. Trends Endocrinol. Metab. **23:**582–590. http://dx.doi.org/10.1016/j.tem.2012.05.005.
14. **Kuroda Y, Matsuo K.** 2012. Molecular mechanisms of triggering, amplifying and targeting RANK signaling in osteoclasts. World J. Orthop. **3:**167–174. http://dx.doi.org/10.5312/wjo.v3.i11.167.
15. **Kobayashi N, Kadono Y, Naito A, Matsumoto K, Yamamoto T, Tanaka S, Inoue J.** 2001. Segregation of TRAF6-mediated signaling pathways clarifies its role in osteoclastogenesis. EMBO J. **20:**1271–1280. http://dx.doi.org/10.1093/emboj/20.6.1271.
16. **Takayanagi H, Kim S, Koga T, Nishina H, Isshiki M, Yoshida H, Saiura A, Isobe M, Yokochi T, Inoue J, Wagner EF, Mak TW, Kodama T, Taniguchi T.** 2002. Induction and activation of the transcription factor

NFATc1 (NFAT2) integrate RANKL signaling in terminal differentiation of osteoclasts. Dev. Cell **3:**889–901. http://dx.doi.org/10.1016/S1534-5807(02)00369-6.
17. **Franzoso G, Carlson L, Xing L, Poljak L, Shores EW, Brown KD, Leonardi A, Tran T, Boyce BF, Siebenlist U.** 1997. Requirement for NF-kappaB in osteoclast and B-cell development. Genes Dev. **11:** 3482–3496. http://dx.doi.org/10.1101/gad.11.24.3482.
18. **Wagner EF, Eferl R.** 2005. Fos/AP-1 proteins in bone and the immune system. Immunol. Rev. **208:**126–140. http://dx.doi.org/10.1111/j.0105-2896.2005.00332.x.
19. **Wu M, Deng L, Zhu G, Li Y-P.** 2010. G protein and its signaling pathway in bone development and disease. Front. Biosci. (Landmark Ed) **15:** 957–985. http://dx.doi.org/10.2741/3656.
20. **Greenfield EM.** 2012. Anabolic effects of intermittent PTH on osteoblasts. Curr. Mol. Pharmacol. **5:**127–134. http://dx.doi.org/10.2174/1874-470211205020127.
21. **Darveau RP.** 2010. Periodontitis: a polymicrobial disruption of host homeostasis. Nat. Rev. Microbiol. **8:**481–490. http://dx.doi.org/10.1038/nrmicro2337.
22. **Siegert P, Schmidt G, Papatheodorou P, Wieland T, Aktories K, Orth JHC.** 2013. *Pasteurella multocida* toxin prevents osteoblast differentiation by transactivation of the MAP-kinase cascade via the Gα(q/11)—p63RhoGEF—RhoA axis. PLoS Pathog. **9:**e1003385. http://dx.doi.org/10.1371/journal.ppat.1003385.
23. **Collin-Osdoby P, Osdoby P.** 2012. RANKL-mediated osteoclast formation from murine RAW 264.7 cells. Methods Mol. Biol. **816:**187–202. http://dx.doi.org/10.1007/978-1-61779-415-5_13.
24. **Kamitani S, Ao S, Toshima H, Tachibana T, Hashimoto M, Kitadokoro K, Fukui-Miyazaki A, Abe H, Horiguchi Y.** 2011. Enzymatic actions of *Pasteurella multocida* toxin detected by monoclonal antibodies recognizing the deamidated α subunit of the heterotrimeric GTPase Gq. FEBS J. **278:**2702–2712. http://dx.doi.org/10.1111/j.1742-4658.2011.08197.x.
25. **Lee SH, Rho J, Jeong D, Sul JY, Kim T, Kim N, Kang JS, Miyamoto T, Suda T, Lee SK, Pignolo RJ, Koczon-Jaremko B, Lorenzo J, Choi Y.** 2006. V-ATPase V0 subunit d2-deficient mice exhibit impaired osteoclast fusion and increased bone formation. Nat. Med. **12:**1403–1409.
26. **Malumbres M, Barbacid M.** 2003. RAS oncogenes: the first 30 years. Nat. Rev. Cancer **3:**459–465. http://dx.doi.org/10.1038/nrc1097.
27. **Wilson BA, Ho M.** 2012. *Pasteurella multocida* toxin interaction with host cells: entry and cellular effects. Curr. Top. Microbiol. Immunol. **361:** 93–111. http://dx.doi.org/10.1007/82_2012_219.
28. **Hollinger S, Hepler JR.** 2002. Cellular regulation of RGS proteins: modulators and integrators of G protein signaling. Pharmacol. Rev. **54:** 527–559. http://dx.doi.org/10.1124/pr.54.3.527.
29. **Hepler JR, Berman DM, Gilman AG, Kozasa T.** 1997. RGS4 and GAIP are GTPase-activating proteins for Gq alpha and block activation of phospholipase C beta by gamma-thio-GTP-Gq alpha. Proc. Natl. Acad. Sci. U. S. A. **94:**428–432. http://dx.doi.org/10.1073/pnas.94.2.428.
30. **Girkontaite I, Missy K, Sakk V, Harenberg A, Tedford K, Pötzel T, Pfeffer K, Fischer KD.** 2001. Lsc is required for marginal zone B cells, regulation of lymphocyte motility and immune responses. Nat. Immunol. **2:**855–862. http://dx.doi.org/10.1038/ni0901-855.
31. **Sallese M, Mariggiò S, D'Urbano E, Iacovelli L, De Blasi A.** 2000. Selective regulation of Gq signaling by G protein-coupled receptor kinase 2: direct interaction of kinase N terminus with activated Galphaq. Mol. Pharmacol. **57:**826–831. http://dx.doi.org/10.1124/mol.57.4.826.
32. **Nishimura A, Kitano K, Takasaki J, Taniguchi M, Mizuno N, Tago K, Hakoshima T, Itoh H.** 2010. Structural basis for the specific inhibition of heterotrimeric Gq protein by a small molecule. Proc. Natl. Acad. Sci. U. S. A. **107:**13666–13671. http://dx.doi.org/10.1073/pnas.1003553107.
33. **Takasaki J, Saito T, Taniguchi M, Kawasaki T, Moritani Y, Hayashi K, Kobori M.** 2004. A novel Galphaq/11-selective inhibitor. J. Biol. Chem. **279:**47438–47445. http://dx.doi.org/10.1074/jbc.M408846200.
34. **Souchet M, Portales-Casamar E, Mazurais D, Schmidt S, Léger I, Javré JL, Robert P, Berrebi-Bertrand I, Bril A, Gout B, Debant A, Calmels TP.** 2002. Human p63RhoGEF, a novel RhoA-specific guanine nucleotide exchange factor, is localized in cardiac sarcomere. J. Cell Sci. **115**(Pt 3): 629–640.
35. **Birnbaumer L.** 2007. The discovery of signal transduction by G proteins: a personal account and an overview of the initial findings and contributions that led to our present understanding. Biochim. Biophys. Acta **1768:** 756–771. http://dx.doi.org/10.1016/j.bbamem.2006.09.027.
36. **Rozengurt E.** 2007. Mitogenic signaling pathways induced by G protein-coupled receptors. J. Cell. Physiol. **213:**589–602. http://dx.doi.org/10.1002/jcp.21246.
37. **Andreev J, Galisteo ML, Kranenburg O, Logan SK, Chiu ES, Okigaki M, Cary LA, Moolenaar WH, Schlessinger J.** 2001. Src and Pyk2 mediate G-protein-coupled receptor activation of epidermal growth factor receptor (EGFR) but are not required for coupling to the mitogen-activated protein (MAP) kinase signaling cascade. J. Biol. Chem. **276:**20130–20135. http://dx.doi.org/10.1074/jbc.M102307200.
38. **Roelle S, Grosse R, Buech T, Chubanov V, Gudermann T.** 2008. Essential role of Pyk2 and Src kinase activation in neuropeptide-induced proliferation of small cell lung cancer cells. Oncogene **27:**1737–1748. http://dx.doi.org/10.1038/sj.onc.1210819.
39. **Ray BJ, Thomas K, Huang CS, Gutknecht MF, Botchwey EA, Bouton AH.** 2012. Regulation of osteoclast structure and function by FAK family kinases. J. Leukoc. Biol. **92:**1021–1028. http://dx.doi.org/10.1189/jlb.0512259.
40. **Itzstein C, Coxon FP, Rogers MJ.** 2011. The regulation of osteoclast function and bone resorption by small GTPases. Small GTPases **2:**117–130. http://dx.doi.org/10.4161/sgtp.2.3.16453.
41. **De Jong MF, Nielsen JP.** 1990. Definition of progressive atrophic rhinitis. Vet. Rec. **126:**93.
42. **Mullan PB, Lax AJ.** 1998. *Pasteurella multocida* toxin stimulates bone resorption by osteoclasts via interaction with osteoblasts. Calcif. Tissue Int. **63:**340–345. http://dx.doi.org/10.1007/s002239900537.
43. **Hildebrand D, Heeg K, Kubatzky KF.** 2011. *Pasteurella multocida* toxin-stimulated osteoclast differentiation is B cell dependent. Infect. Immun. **79:**220–228. http://dx.doi.org/10.1128/IAI.00565-10.
44. **Asagiri M, Sato K, Usami T, Ochi S, Nishina H, Yoshida H, Morita I, Wagner EF, Mak TW, Serfling E, Takayanagi H.** 2005. Autoamplification of NFATc1 expression determines its essential role in bone homeostasis. J. Exp. Med. **202:**1261–1269. http://dx.doi.org/10.1084/jem.20051150.
45. **Wilson BA, Zhu X, Ho M, Lu L.** 1997. *Pasteurella multocida* toxin activates the inositol triphosphate signaling pathway in Xenopus oocytes via G(q)alpha-coupled phospholipase C-beta1. J. Biol. Chem. **272:** 1268–1275. http://dx.doi.org/10.1074/jbc.272.2.1268.
46. **Knowles HJ, Athanasou NA.** 2009. Canonical and non-canonical pathways of osteoclast formation. Histol. Histopathol. **24:**337–346.
47. **Hanyu R, Wehbi VL, Hayata T, Moriya S, Feinstein TN, Ezura Y, Nagao M, Saita Y, Hemmi H, Notomi T, Nakamoto T, Schipani E, Takeda S, Kaneko K, Kurosawa H, Karsenty G, Kronenberg HM, Vilardaga JP, Noda M.** 2012. Anabolic action of parathyroid hormone regulated by the β2-adrenergic receptor. Proc. Natl. Acad. Sci. U. S. A. **109:**7433–7438. http://dx.doi.org/10.1073/pnas.1109036109.
48. **Ludwig MG, Vanek M, Guerini D, Gasser JA, Jones CE, Junker U, Hofstetter H, Wolf RM, Seuwen K.** 2003. Proton-sensing G-protein-coupled receptors. Nature **425:**93–98. http://dx.doi.org/10.1038/nature01905.
49. **Yang M, Mailhot G, Birnbaum MJ, MacKay CA, Mason-Savas A, Odgren PR.** 2006. Expression of and role for ovarian cancer G-protein-coupled receptor 1 (OGR1) during osteoclastogenesis. J. Biol. Chem. **281:** 23598–23605. http://dx.doi.org/10.1074/jbc.M602191200.
50. **Whyte LS, Ryberg E, Sims NA, Ridge SA, Mackie K, Greasley PJ, Ross RA, Rogers MJ.** 2009. The putative cannabinoid receptor GPR55 affects osteoclast function in vitro and bone mass in vivo. Proc. Natl. Acad. Sci. U. S. A. **106:**16511–16516. http://dx.doi.org/10.1073/pnas.0902743106.
51. **Iwai K, Koike M, Ohshima S, Miyatake K, Uchiyama Y, Saeki Y, Ishii M.** 2007. RGS18 acts as a negative regulator of osteoclastogenesis by modulating the acid-sensing OGR1/NFAT signaling pathway. J. Bone Miner. Res. **22:**1612–1620. http://dx.doi.org/10.1359/jbmr.070612.
52. **Orth JHC, Lang S, Taniguchi M, Aktories K.** 2005. *Pasteurella multocida* toxin-induced activation of RhoA is mediated via two families of G{alpha} proteins, G{alpha}q and G{alpha}12/13. J. Biol. Chem. **280:**36701–36707. http://dx.doi.org/10.1074/jbc.M507203200.
53. **Guttenberg G, Hornei S, Jank T, Schwan C, Lü W, Einsle O, Papatheodorou P, Aktories K.** 2012. Molecular characteristics of Clostridium perfringens TpeL toxin and consequences of mono-O-GlcNAcylation of Ras in living cells. J. Biol. Chem. **287:**24929–24940. http://dx.doi.org/10.1074/jbc.M112.347773.
54. **Busch C, Orth J, Djouder N, Aktories K.** 2001. Biological activity of a C-terminal fragment of *Pasteurella multocida* toxin. Infect. Immun. **69:** 3628–3634. http://dx.doi.org/10.1128/IAI.69.6.3628-3634.2001.